RESEARCH ARTICLE

Macromolecular Reaction Engineering
www.mre-journal.de

Forces Driving the Development of Particle Morphology of Waterborne Polymer Dispersions

Hesham Abdeldaim and José M. Asua**

Particle morphology is a key characteristic of the waterborne polymer dispersions and plenty of effort has been dedicated to understand the mechanisms controlling the development of the morphology during polymerization. The availability of new characterization techniques that provide unprecedented quantitative details of the particle morphology have questioned the ideas about the driving forces ruling the development of the morphology. In this article, the case is considered of a seeded emulsion polymerization in which the second stage polymer (Polymer 2) is more hydrophobic than the seed polymer and a water-soluble initiator is used. Simulations of the effect of the different forces involved in the formation of the particle morphology carried by integrating the Navier–Stokes are compared with available experimental results. If is found that the interfacial tensions are responsible for the penetration of clusters of polymer 2 within the seed polymer and the spread of these clusters over the surface of the particle. On the other hand, van der Waals forces control coalescence of the clusters both at the surface and in the interior of the particle.

1. Introduction

Particle morphology is a key characteristic of the waterborne dispersions.[1–3] As these are product-by-process materials, plenty of effort has been devoted to understand the mechanisms controlling the development of the morphology during polymerization, both experimentally and by modelling approaches.[4–18] The final goal is to develop optimization and control strategies of the particle morphology. At first sight, this seems an almost impossible task because particle morphology is neither measurable nor observable on-line. Nevertheless, this is not a completely new situation in polymer reaction engineering because using reaction calorimetry as the only on line measurement, copolymer composition[19,20] and molar mass distributions (MMD) of linear polymers[21,22] (both nonobservable from calorimetric measurements) have been controlled. In both cases, the solution was to use a mathematical model that was able to estimate the state variables (copolymer composition and MMD) from the measurable variable (heat of reaction).

With this idea in mind, we have developed a mathematical model for the development of the particle morphology.[23] This model presents two advantages with respect to the previous models. The first one is that the morphology of the whole latex is described by using cluster distributions, whereas in the previous models[5–7,9,13] the morphology of a single particle was calculated. The second one is that it is much more efficient computationally, which is a necessary condition for optimization and on-line control. The model has been validated for polymer–polymer[24] and polymer–inorganic[25] systems. In both cases, the validation was based on the good agreement between the predictions of the model and the images of the particle morphology obtained by conventional transmission electron microscopy (TEM) using stained samples, which was good. The model was also used to perform optimizations in silico[26] finding that the optimum trajectories were not obvious even for a person skilled in the art, which highlights the benefits of the mathematical model. The possibility of using the model as a soft sensor for online control of the particle morphology has also been explored in silico.[27] Very recently, the model has been used to demonstrate in silico the existence of master curves that can be used for the online control of particle morphology. This conclusion has been supported by experimental data.[28]

High angle annular dark field- scanning transmission electron microscopy (HAADF-STEM) has been used for the characterization of the particle morphology.[29] This HAADF-STEM technique provides unprecedented quantitative details about the particle morphology development. The technique was applied to composite latexes obtained in seeded semicontinuous emulsion polymerizations initiated with a water-soluble initiator. In these experiments, the seed was more hydrophilic than the second stage monomer and hence the equilibrium morphology was an inverted core–shell with the second stage hydrophobic polymer (Polymer 2) in the core and the seed polymer (Polymer 1) in the shell.[30] However, as illustrated in **Figure 1** for the case in which the glass transition temperature of the polymer forming the seed

H. Abdeldaim, J. M. Asua
POLYMAT, Kimika Aplikatu saila, Kimika Fakultatea
University of the Basque Country UPV/EHU
Avda Tolosa 72, Donostia-San Sebastián 20018, Spain
E-mail: hesham.ahmed@eng.asu.edu.eg; jm.asua@ehu.eus

The ORCID identification number(s) for the author(s) of this article can be found under https://doi.org/10.1002/mren.202100038

DOI: 10.1002/mren.202100038

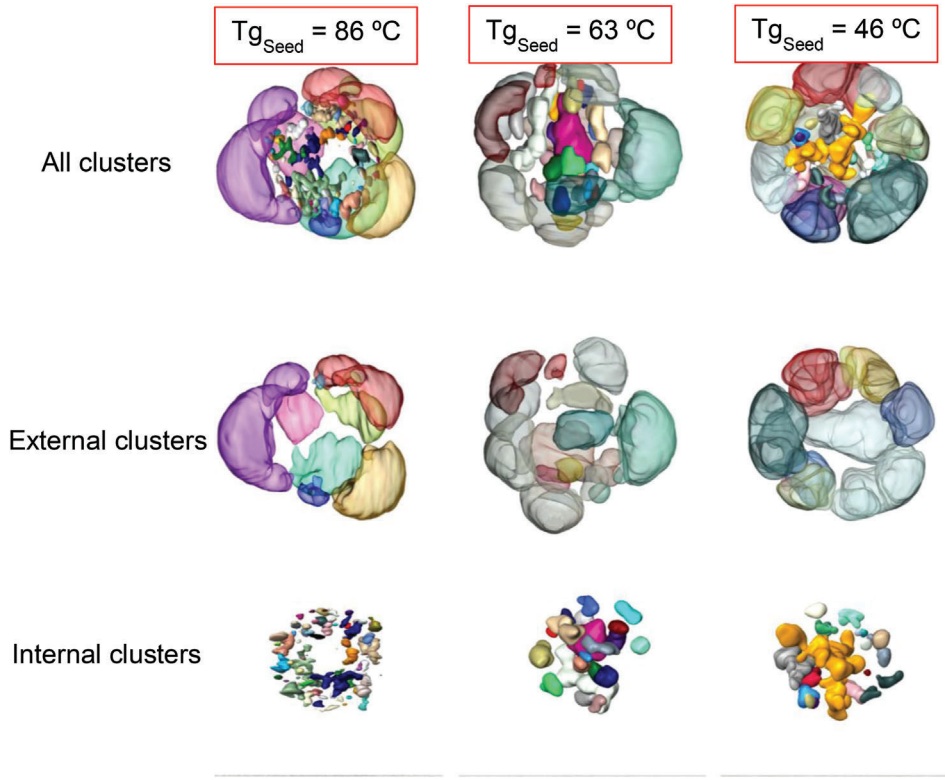

Figure 1. Effect of the T_g of the seed on the final particle morphology of latexes obtained in seeded semicontinuous emulsion polymerization (Seed: MMA/BA/AA/AM; 2nd stage: S/BA/AA/AM (T_g = 45 °C); Polymerization temperature = 80 °C; Initiator: TBHP/ACBS).[29] Adapted with permission from Rajabalinia et al. *Macromolecules* 2019, *52*, 5298–5306. Copyright (2019) American Chemical Society.

(Polymer 1) was varied, the images obtained by HAADF-STEM show a completely different morphology, with most of Polymer 2 either sitting on or partially embedded in the surface of the particle. The higher the difference between the polymerization temperature and the effective glass transition temperature of the seed (i.e., taking into account the T_g of the seed polymer and the plasticization effect of the monomer) the more embedded the clusters of Polymer 2. The preferential formation of Polymer 2 near the surface of the particle was attributed to the radical concentration profile formed as a consequence of the use of a water soluble initiator. Actually, the experimental results available for the evolution of the particle morphology during the seeded semicontinuous emulsion polymerization[24] show that, initially, many small clusters of Polymer 2 were formed on the surface of the particle and that later they grew by polymerization and coagulation, undergoing at the same time some penetration into the polymer particle (**Figure 2**). The higher degree of penetration of the surface clusters into softer particles can be attributed to the lower resistance that the polymer in the seed opposed to the migration of the clusters towards the equilibrium morphology (inverted core–shell). Analysis of the final samples by HAADF-STEM (Figure 1) shows that small clusters appeared in the interior of the particle, whose origin was attributed to monomeric radicals formed by chain transfer to monomer that diffused towards the interior of the particle. As the T_g of the seed was reduced, it was expected that these clusters would move towards the center of the particle (equilibrium morphology). Surprisingly, it was found that this was not the case, and the amount of Polymer 2 that stayed in the interior of the particle decreased when the T_g of Polymer 1 was lower than a certain value. This observation was attributed to the attractive van der Waals forces between the small interior clusters and large ones near the surface.[29]

These findings made us beware of our ideas on the driving forces for the development of the particle morphology that were the base of our model and that can be summarized as follows. Polymer 2 is formed within the polymer particle accordingly to the radical concentration profile. Clusters are formed when the concentration of the newly formed Polymer 2 exceeded the solubility limit. These clusters grow by polymerization, and coagulate between them and move towards the equilibrium morphology due to repulsive van der Waals forces with the aqueous phase.

However, the results in Figure 1 challenge this view. First, clusters are formed at the surface of the particles. Second, there are no repulsive van der Waals forces between the clusters located on the particle surface and the aqueous phase to push them towards the interior of the particle. Third, interior clusters seemed to move away from the equilibrium. Therefore, the driving forces have to be reconsidered.

In this article, the forces involved in the formation of the particle morphology are analyzed and the effect of these forces on the movement of the clusters is simulated by integrating the Navier–Stokes equation by using COMSOL Multiphysics. It is shown that these forces can justify the HAADF-STEM observations, which means that they are the significant ones.

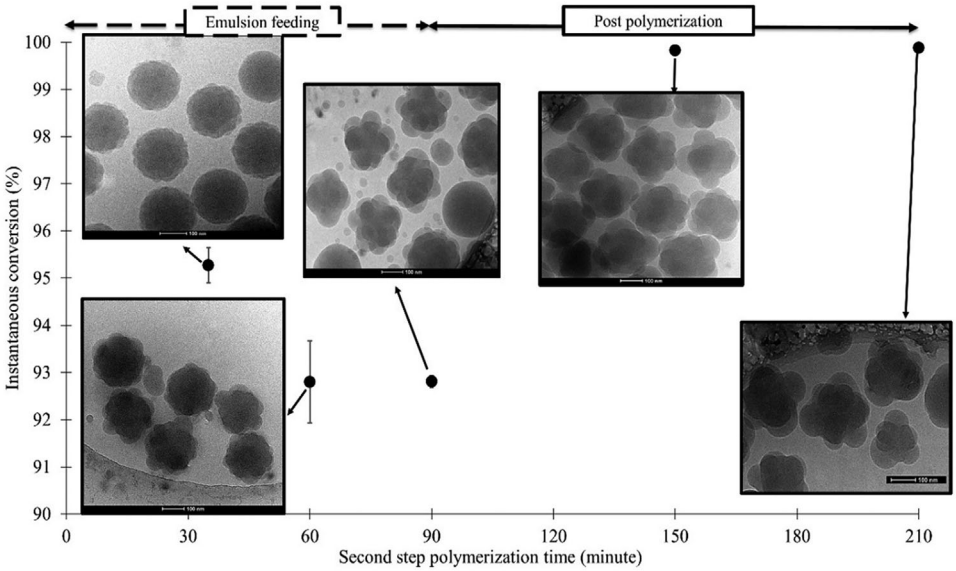

Figure 2. Evolution of the particle morphology during the seeded semicontinuous emulsion polymerization of methyl methacrylate/butyl acrylate/acrylic acid/acrylamide ($T_{gPolymer2} = 45$ °C) on a methyl methacrylate/butyl acrylate/acrylic acid/acrylamide seed ($T_{gPolymer1} = 80$ °C). Reprinted from Chemical Engineering Journal, 363, Rajabalinia et al. Experimental Validation of a Mathematical Model for the Evolution of the Particle Morphology of Waterborne Polymer-Polymer Hybrids: Paving the Way to the Design and Implementation of Optimal Polymerization Strategies. 259–269. Copyright (2019) with permission from Elsevier.

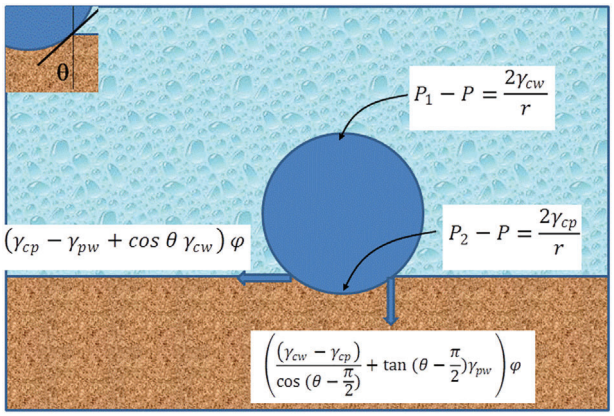

Figure 3. Forces and pressures acting on the clusters placed at the surface of the particles. *P* is the pressure in the aqueous phase.

2. Driving Forces for the Development of the Particle Morphology

In this section, the forces acting on the clusters located at the surface of the polymer particle and within the polymer particle are discussed.

2.1. Forces Acting on a Cluster Located at the Surface of the Polymer Particle

Let us consider the situation depicted in **Figure 3** where for the sake of the discussion, the cluster is considered spherical and the surface of the particle is represented as a flat surface. The significant variables are the interfacial tensions between the cluster and the aqueous phase (γ_{cw}), the cluster and the polymer particle (γ_{cp}) and the particle and the aqueous phase (γ_{pw}). For the current system, the equilibrium morphology is the inverted core–shell, and hence[30]

$$\gamma_{cw} > \gamma_{cp} + \gamma_{pw}\ [\mathrm{Jm^{-2}}] \tag{1}$$

Under these conditions, the cluster will move towards the interior of the particle. The force driving this movement can be calculated as the derivative of the surface energy, and it is given by (Equation S4, Supporting Information)

$$F = \left(\frac{(\gamma_{cw} - \gamma_{cp})}{\cos\left(\theta - \frac{\pi}{2}\right)} + \tan\left(\theta - \frac{\pi}{2}\right)\gamma_{pw}\right)\varphi\ [\mathrm{N}] \tag{2}$$

where θ is the contact angle shown in Figure 3 and φ is the perimeter of the three-phase line. This force should overcome the viscous drag. Therefore, the higher the effective viscosity of the seed polymer (that increases with the T_g of the seed polymer) the lower the penetration as observed in Figure 1.

On the other hand, the HAADF-STEM results show that when the T_g of the seed is high and the clusters could not penetrate in the particle, they wetted the surface of the polymer particle. The wetting force can be approximated by[31]

$$F = (\gamma_{pw} - \gamma_{cp} - \cos\theta\ \gamma_{cw})\quad \varphi\ [N] \tag{3}$$

In addition, the differences in interfacial tensions create a difference of pressure inside the cluster that can be calculated by means of the Young–Laplace equation. The forces and pressures are included in Figure 2. It is worth to point out that while subjected to these forces, the volume of the cluster grows by polymerization.

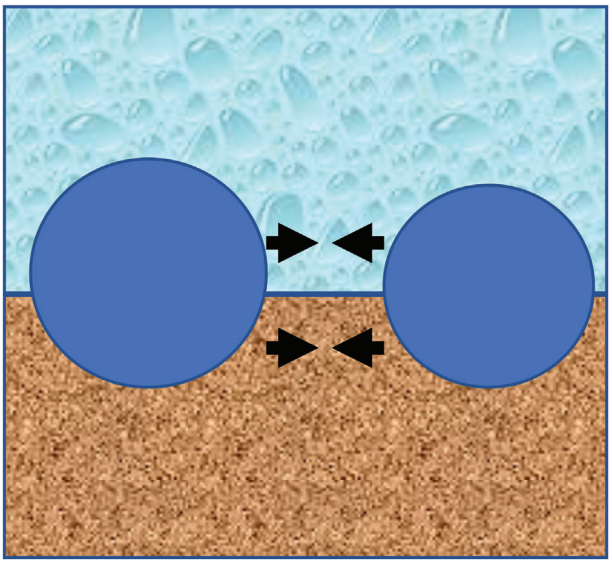

Figure 4. Van der Waals forces on clusters located at the surfaced of the particle. The equations are given in the Supporting Information.

So far, only one isolated cluster has been considered. However, the experimental results[24] show that the surface of the particle is covered by many clusters. Therefore, the interaction between them should be considered. In addition to the forces depicted in Figure 3, the two clusters in **Figure 4** are affected by attractive var der Waals forces through both the aqueous phase and polymer particle. These forces are proportional to the effective Hamaker constants[32] and to the mass of the clusters in contact with the aqueous phase and the polymer particle. As the Hamaker constant is proportional to the interfacial tensions and $\gamma_{cw} > \gamma_{cp}$, the van der Waals force per unit mass is greater through the aqueous phase. In addition, the viscosity of the water phase is negligible. Therefore, the coalescence is expected to occur through the aqueous phase. However, the fractions of the clusters that penetrate into the particle anchor the clusters to the particles and hence the coalescence will occur by deformation of the clusters, where the main resistance is the viscoelasticity of the clusters.

2.2. Forces Acting on Clusters Located Inside of the Polymer Particle

The clusters that are inside the polymer particles are subjected to van der Waals forces. For the system discussed in this article (second stage polymer more hydrophobic than the seed polymer) the forces are repulsive between the cluster and the aqueous phase and attractive between clusters. It has been estimated[29] that for viscosities in the range of 10^5 Pa s, the effect of the van der Waals forces is significant for distances up to about 15–20 nm. A look to Figure 1 shows that the interior clusters were at more than 15 nm from the aqueous phase, therefore it is unlikely that they were significantly affected by the repulsive forces with the aqueous phase. On the other hand, the internal clusters were relatively close to the clusters placed at the surface of the particles and are attracted by them. This attractive force as well as the one between spherical internal clusters are calculated in the Supporting Information.

Table 1. Values of the parameters used in the mechanical model.

γ_{cw}	10 [mN m^{-1}]
γ_{cp}	7 [mN m^{-1}]
γ_{pw}	2 [mN m^{-1}]
A_{cwc}	4.2E-21 [J]
A_{cpc}	2.94E-21 [J]

3. Cluster Movement

In the previous section, the forces acting on the clusters are discussed. However, their direct use in the calculation of the movement of the clusters is complicated by the fact that the shape of the clusters varies with time. This problem was overcome by calculating the movement of the clusters using the Navier–Stokes equation (Equation 4) coupled with the continuity equation (Equation 5)

$$\rho\frac{\partial u}{\partial t} + \rho\,(u.\nabla)\,u = \nabla.\left[-PI + \eta\left(\left(\nabla u + \nabla u^{T}\right)\right)\right] + F_{st}\left[\mathrm{Nm^{-3}}\right] \quad (4)$$

$$\nabla\,.\,u = 0\left[\mathrm{s^{-1}}\right] \quad (5)$$

where, ρ is the density, u is the flow velocity, t represents the time, P is the pressure, η denotes the dynamic viscosity, and F_{st} is the force per unit volume due to interfacial tension given by[33]

$$F_{st} = \sigma\delta\kappa n + \delta\nabla_{s}\sigma \quad (6)$$

where, σ is the interfacial tension, n is the unit normal to the interface, $\kappa = -\nabla\, n$ is the curvature.

The Navier–Stokes equations were solved by finite elements using COMSOL Multiphysics platform based on the creeping two-phase flow level-set interface coupled with the electrostatic interface and deformed geometry modules. The software automatically calculates the forces due to the interfacial tensions adapting the calculation to the evolving shape of the clusters. First, the penetration of a cluster into the seed particle was calculated. The initial state for the simulation was a spherical cluster of 30 nm in diameter placed on the surface of a spherical particle. It was considered that both Polymer 1 (seed polymer) and Polymer 2 (clusters) were viscoelastic materials that could be represented by the Maxwell model.[34] As the movement of the clusters is very slow, only the viscous part plays a role, and therefore the behavior of the system can be described by the viscosity of the two phases.

Figures 5 and **6** present the effect of the viscosities of the seed polymer and the cluster on the penetration of a cluster into the particle. The parameters used in the simulation are presented in **Table 1**. It can be seen that for a relatively soft cluster ($\eta = 10^6$ Pa s), when the viscosity of the seed polymer was high ($\eta = 10^9$ Pa s) the cluster did not penetrate and spread on the surface of the particle. For a lower viscosity of the seed polymer ($\eta = 10^8$ Pa s), the cluster penetrates into the seed, but after 400 s still is in contact with the aqueous phase. For an even lower viscosity ($\eta = 10^6$ Pa s), the cluster completely penetrates into the seed in 400 s. Comparison with the images in Figure 1 shows that the model

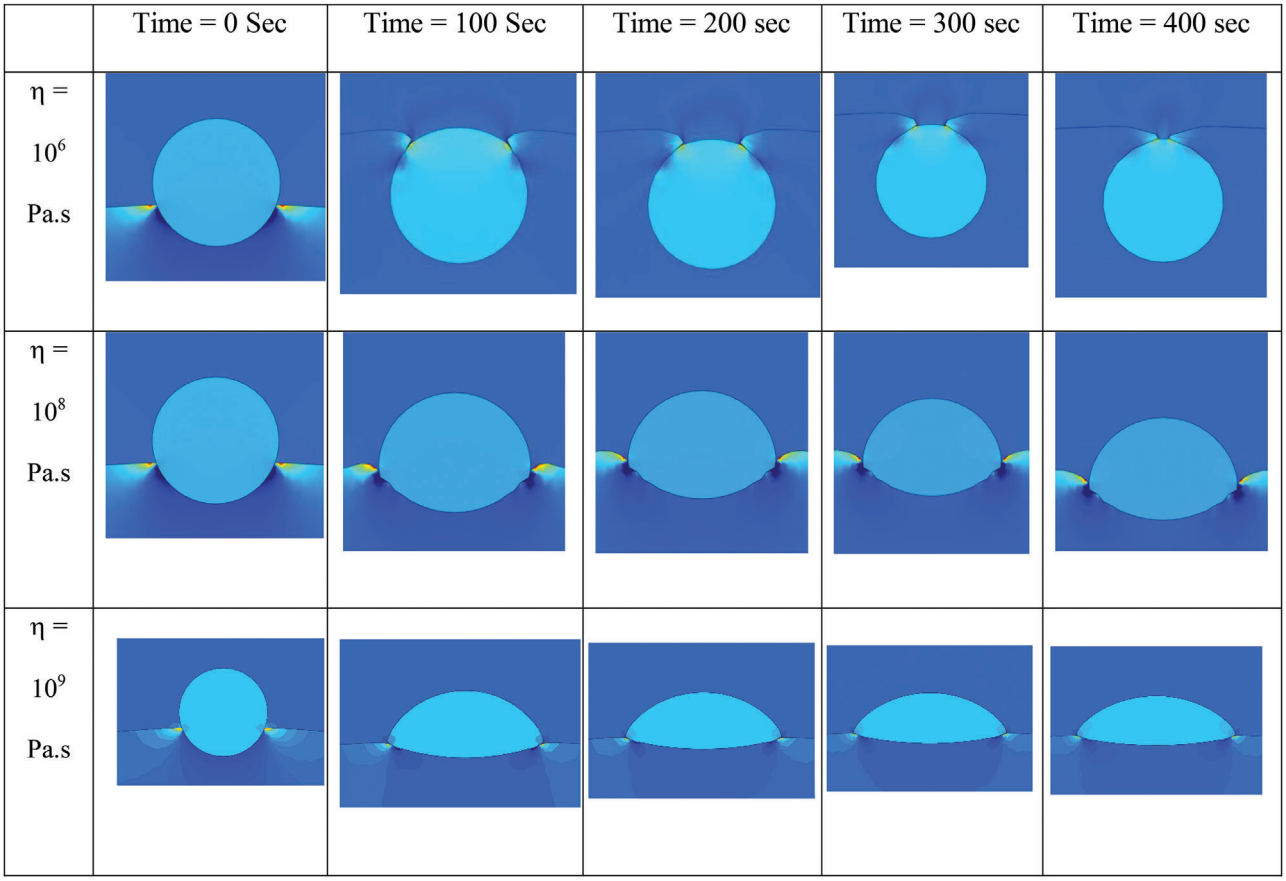

Figure 5. Effect of the viscosity of Polymer 1 (seed polymer) on the on the penetration of a cluster of viscosity ($\eta_{Polymer2} = 10^6$ Pas) into the particle. Diameter of the cluster: 30 nm; Position at $t = 0$: 10 nm inside the seed polymer (20 nm outside).

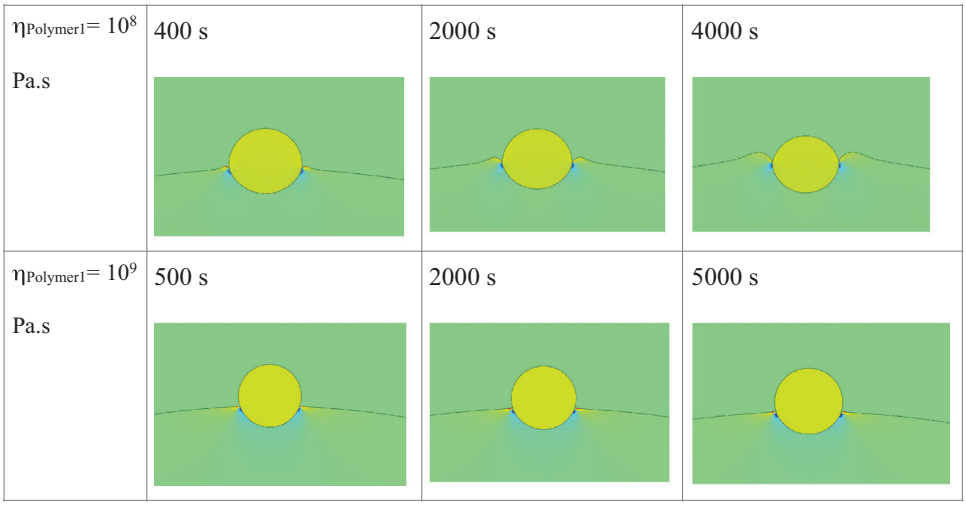

Figure 6. Effect of the viscosity of Polymer 1 (seed polymer) on the on the penetration of a cluster of viscosity ($\eta_{Polymer2} = 10^8$ Pa s) into the particle. Diameter of the cluster: 30 nm; Position at $t = 0$: 10 nm inside the seed polymer (20 nm outside).

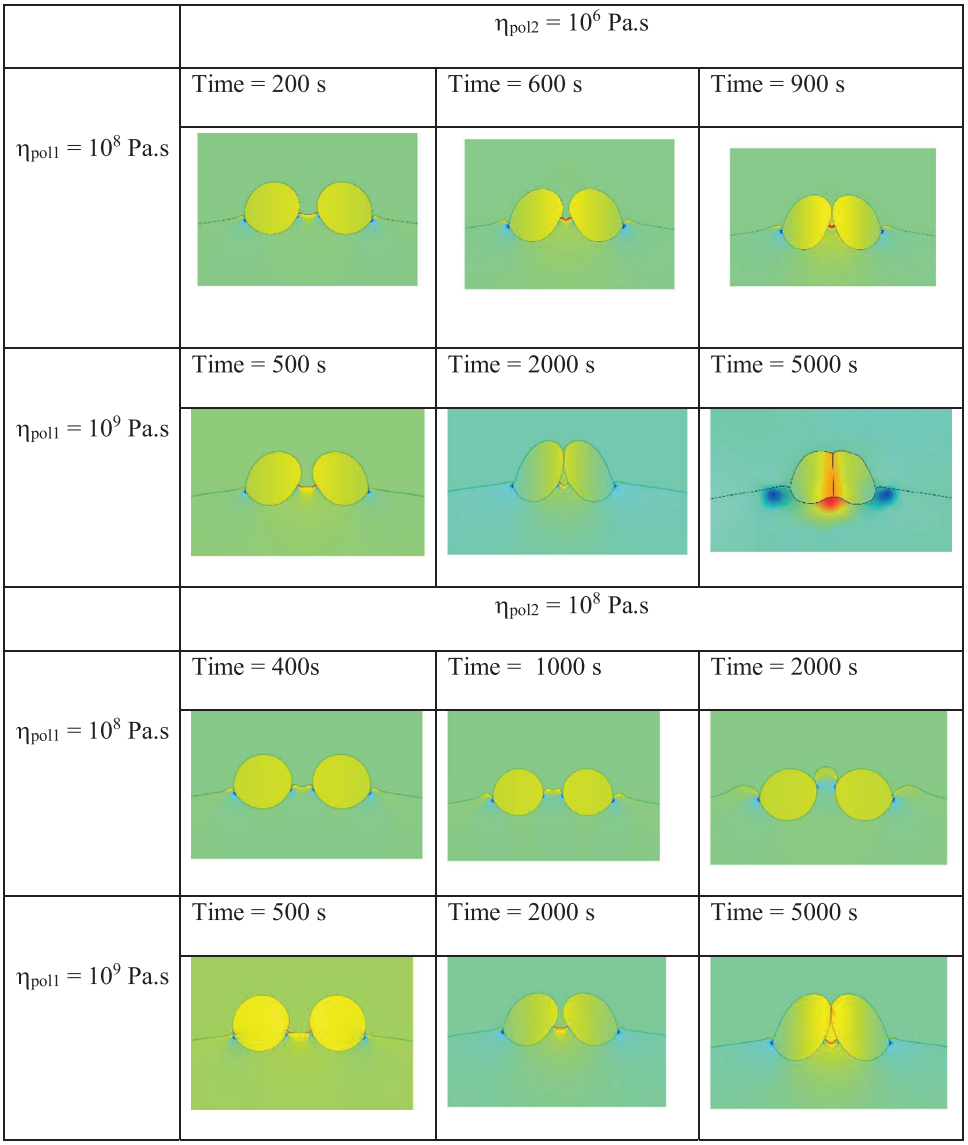

Figure 7. Coagulation of surface clusters. Initial situation: 30 nm clusters that have 10 nm inside the seed polymer. The initial distance between the surfaces of the clusters was 12 nm.

describes well the experimental observations, with the case of the highest viscosity corresponding to the experiment with T_{gseed} = 86 °C and the case with the intermediate viscosity representing the other T_{gs}. No complete penetration of the clusters was observed in the experiments presented in Figure 1, which indicates a viscosity higher than $\eta = 10^6$ Pa s. From this study it can be concluded that the penetration of the hydrophobic clusters formed at the surface of the particles is due to the effect of the interfacial tensions.

Comparison between Figures 5 and 6 illustrates the effect of the relative values of the viscosities of the cluster and seed polymer. The higher the viscosity of the cluster the deeper penetrates into the seed. The reason is that hard clusters deform less and therefore maintain a spherical shape that presents less area perpendicular to the movement of the cluster than flattened clusters (shape characteristic of low viscosity clusters).

The coagulation of surface clusters was considered next. The initial situation was that presented in Figure 4 with clusters of 30 nm in diameter that have 10 nm inside the seed polymer. The initial distance between the surfaces of the clusters was 12 nm. The van der Waals forces (Equations S6 and S7, Supporting Information) were included manually into the Navier–Stokes equation. The Hamaker constants (A_{ijk}) used are given in Table 1. The viscosities considered were: $\eta_{pol2} = 10^6$ and 10^8 Pa s and $\eta_{pol1} = 10^8$ and 10^9 Pa s. **Figure 7** shows that there is a competition between penetration and coalescence. Soft clusters are more prone to coalesce because on one hand they penetrate less and on the other they are deform easier through the aqueous phase. For example, in a 10^8 Pa s seed, 10^6 Pa s viscous clusters remained at the surface and underwent coalescence, whereas 10^8 Pa s clusters penetrate within the particle before suffering any deformation along the surface of the particle.

4. Summary of the Driving Forces Ruling the Evolution of the Particle Morphology

Combination of the experimental observations with the simulations of the mechanical model provides a quite complete image of the development of the particle morphology. In the initial stages of the seeded semicontinuous emulsion polymerization using a water soluble initiator, plenty of clusters of Polymer 2 are formed at the surface of the particles. This indicates that most of radicals are retained next to the surface. These clusters grow by polymerization and undergo coalescence driven by the combination of forces resulting from the interfacial tensions (Figure 3) and the van der Waals forces depicted in Figure 4. The effective viscosities (viscosities including the plasticization due to monomer and water) of the seed polymer and clusters oppose to this movement. Nucleation of new clusters at the surface of the particle decreases with time because the area occupied by the clusters increases. Surface clusters are pushed towards the interior of the particle by the effect of the interfacial tensions (Equation 2). Resistance to this movement is due to the effective viscosity of the seed polymer. Penetration is also affected by the viscosity of the cluster. Hard clusters maintain their sphericity whereas soft clusters are flattened. The result of that the area perpendicular to the movement and consequently the drag force is less for hard cluster, which penetrate deeper. In addition, wetting of the surface of the particle by Polymer 2 occurs due to the combined effect of Equation (3) and the pressure differences illustrated in Figure 3. Furthermore, clusters at the surface of the particles can coagulate between them. The driving force for the coagulation is the van der Waals attractive force between the fraction of the clusters that protrude above the surface. The viscoelasticity of the cluster opposes the movement. The relative rates of surface coalescence and penetration determine the fate of the cluster. In general, the harder the cluster the more likely that it will penetrate in the particle. Once the external clusters are completely embedded in the seed polymer, they are not affected by the interfacial forces (Equations (2) and (3)) and they are subjected to repulsive van der Waals forces from the aqueous phase (Equation S5 and S7, Supporting Information) as well as to attractive van der Waals forces with the other clusters. The effect of these repulsive–attractive van der Waals forces on the movement of the clusters is strongly dependent on the effective viscosity of the seed polymer as well as on the particle morphology. For highly viscous seeds, clusters will only penetrate a small distance.

Monomeric radicals formed by chain transfer to monomer can diffuse to the interior of the particle and form clusters. These clusters can undergo coalescence among them as well as with the embedded surface clusters.

A conclusion that may be mistakenly drawn from the discussion above is that the equilibrium core–shell morphology is not attainable. This is not the case for particles smaller than 200 nm with moderate viscosities and a fraction of Polymer 2 in the range of 50%. Under these conditions, clusters will penetrate in the polymer particle, coalescence of the internal clusters will lead to the formation of a single internal cluster that the repulsion between the internal cluster and the aqueous phase will place the cluster at the center of the particle.

The discussion above focuses on a system where the second stage polymer is more hydrophobic than the seed polymer. In the reverse case, the driving forces are those considered above, but the direction of movement will be different. Thus, a cluster that is within the matrix will move towards the exterior driven by van der Waals forces and once it touches the surface, the interfacial forces will bring the whole cluster to the surface and will spread it over the surface.

5. Impact on the Mathematical Modeling of the Development of Particle Morphology

The present work shows that on one part, the driving forces for the movement of the clusters are different from those considered in the available mathematical model for the development of the particle morphology,[23] and that on the other, the movement of the clusters can be well described by integrating the Navier–Stokes equations. Therefore, one might think that the mathematical models should be based on the Navier–Stokes equations. However, this is not possible because the solution of these equations is computationally very demanding and in addition, only the morphology of a single particle will be calculated. Therefore, likely the best option is to use the framework of the existing model,[23] which, based on the population balances of the clusters, provides the evolution of the cluster size distribution, and to use the knowledge gained in this work to calculate the parameters of the model.

6. Conclusions

In this article, the forces driving the development of the particle morphology in a seeded emulsion polymerization where a water soluble initiator is used and the second stage polymer (Polymer 2) is more hydrophobic than the seed polymer. Experimental evidence[24] shows that clusters of Polymer 2 are formed at the surface of the seed. The evolution of these clusters was studied by integrating the Navier–Stokes equations using COMSOL Multiphysics. Both the effect of the interfacial tensions and the van der Waals forces was considered. It was found that the interfacial tensions are responsible for the penetration of clusters of Polymer 2 within the seed polymer and the spread of these clusters over the surface of the particle. On the other hand, van der Waals forces control coalescence of the clusters both at the surface and in the interior of the particle. The simulations agree with the detailed particle morphology observed by HAADF-STEM,[29] indicating that these are the driving forces for the development of the particle morphology. These results shed a new light on the forces driving the development of the particle morphology and will influence future development of mathematical models for this process.

Supporting Information

Supporting Information is available from the Wiley Online Library or from the author.

Acknowledgements

The support of the partners of the Industrial Liaison Program on Polymerization in Disperse Media (Allnex, Akzo-Nobel, Arkema, Asian Paints, BASF, DSM, Elix Polymers, Inovyn, 3M, Stahl, Synthomer, Vinavil, Wacker) is acknowledged.

Conflict of Interest

The authors declare no conflict of interest.

Data Availability Statement

Research data are not shared.

Keywords

interfacial tension, particle morphology, van der Waals forces, waterborne polymers

Received: September 12, 2021
Revised: October 25, 2021
Published online: November 8, 2021

[1] D. C. Sundberg, Y. G. Durant, *Polym. React. Eng.* **2003**, *11*, 379.
[2] Y. Reyes, E. Akhmastkaya, J. R. Leiza, J. M. Asua, in *Chemistry and Technology of Emulsion Polymerisation* (Ed: A. M. van Herk), Wiley, UK **2013**, p. 145.
[3] M. Paulis, J. M. Asua, *Macromol. React. Eng.* **2016**, *10*, 8.
[4] M. Okubo, Y. Katsuta, T. Matsumoto, *J. Polym. Sci., Polym. Lett. Ed.* **1980**, *18*, 481.
[5] L. J. Gonzalez-Ortiz, J. M. Asua, *Macromolecules* **1995**, *28*, 3135.
[6] L. J. González-Ortiz, J. M. Asua, *Macromolecules* **1996**, *29*, 383.
[7] L. J. González-Ortiz, J. M. Asua, *Macromolecules* **1996**, *29*, 383.
[8] O. J. Karlsson, J. M. Stubbs, R. H. Carrier, D. C. Sundberg, *Polym. React. Eng.* **2003**, *11*, 589.
[9] J. Stubbs, R. Carrier, D. C. Sundberg, *Macromol. Theory Simul.* **2008**, *17*, 147.
[10] W. Deng, R. Li, M. Zhang, L. Gong, C. Kan, *J. Colloid Interface Sci.* **2010**, *349*, 122.
[11] V. Herrera, Z. Palmillas, R. Pirri, Y. Reyes, J. R. Leiza, J. M. Asua, *Macromolecules* **2010**, *43*, 1356.
[12] B. Li, Y. Xu, M. Wang, X. Ge, *Langmuir* **2013**, *29*, 14787.
[13] E. Akhmatskaya, J. M. Asua, *Colloid Polym. Sci.* **2013**, *291*, 87.
[14] W. Zhai, B. Wang, Y. Wang, Y.-F. He, P. Song, R.-M. Wang, *Colloids Surf., A* **2016**, *503*, 94.
[15] F. Jasinski, V. L. Teo, R. P. Kuchel, M. Mballa Mballa, S. C. Thickett, R. H. G. Brinkhuis, W. Weaver, P. B. Zetterlund, *Polym. Chem.* **2017**, *8*, 495.
[16] D. Blenner, J. Stubbs, D. Sundberg, *Polymer* **2017**, *114*, 54.
[17] S. Hamzehlou, J. R. Leiza, in *Polymer Reaction Engineering of Dispersed Systems. Adv. Polym. Sci.*, Vol. *281* (Ed: W. Pauer), Springer, Cham **2017**, pp. 105–141.
[18] E. Limousin, N. Ballard, J. M. Asua, *Prog. Org. Coat.* **2019**, *129*, 69.
[19] I. S. De Buruaga, A. Echevarría, P. D. Armitage, J. C. De La Cal, J. R. Leiza, J. M. Asua, *AIChE J.* **1997**, *43*, 1069.
[20] I. Sáenz De Buruaga, P. D. Armitage, J. R. Leiza, J. M. Asua, *Ind. Eng. Chem. Res.* **1997**, *36*, 4243.
[21] M. Vicente, S. Benamor, L. M. Gugliotta, J. R. Leiza, J. M. Asua, *Ind. Eng. Chem. Res.* **2001**, *40*, 218.
[22] M. Vicente, J. R. Leiza, J. M. Asua, *AIChE J.* **2001**, *47*, 1594.
[23] S. Hamzehlou, J. R. Leiza, J. M. Asua, *Chem. Eng. J.* **2016**, *304*, 655.
[24] N. Rajabalinia, S. Hamzehlou, J. R. Leiza, J. M. Asua, *Chem. Eng. J.* **2019**, *363*, 259.
[25] S. Hamzehlou, M. Aguirre, J. R. Leiza, J. M. Asua, *Macromolecules* **2017**, *50*, 7190.
[26] J. M. M. Faust, S. Hamzehlou, J. R. Leiza, J. M. Asua, A. Mhamdi, A. Mitsos, *Chem. Eng. J.* **2019**, *359*, 1035.
[27] J. M. M. Faust, S. Hamzehlou, J. R. Leiza, J. M. Asua, A. Mhamdi, A. Mitsos, *Chem. Eng. J.* **2021**, *414*, 128808.
[28] N. Ballard, W. Gerlinger, J. M. Asua, *Chem. Eng. J.* **2021**, *425*, 131508.
[29] N. Rajabalinia, S. Hamzehlou, E. Modin, A. Chuvilin, J. R. Leiza, J. M. Asua, *Macromolecules* **2019**, *52*, 5298.
[30] Y. C. Chen, V. Dimonie, M. S. El-Aasser, *Pure Appl. Chem.* **1992**, *64*, 1691.
[31] J. C. Berg, *An Introduction to Interfaces and Colloids. The Bridge to Nanotechnology* (Ed: D. Murphy) World Scientific, Singapore **2010**, p. 256.
[32] R. J. Hunter, *Foundations of Colloid Science* (Ed: B. P. Binks). Oxford Science Publications, Oxford, UK **1987**, p. 303.
[33] F. Boyer, C. Lapuerta, S. Minjeaud, B. Piar, M. Quintard, *Transp. Porous Media* **2010**, *82*, 463.
[34] T. A. Osswald, N. Rudolph, *Polymer Rheology: Fundamentals and Applications*, Hanser Publishers, München **2014**.

